

M1 Transition Probabilities in Odd-Mass Deformed Nuclei*

G. G. SEAMAN,† E. M. BERNSTEIN,‡ AND J. M. PALMS§

Los Alamos Scientific Laboratory, University of California, Los Alamos, New Mexico

(Received 17 April 1967)

The odd-mass deformed nuclei ^{158}Eu , ^{159}Tb , ^{165}Ho , ^{169}Tm , ^{175}Lu , and ^{181}Ta have been studied by Coulomb excitation with 50-MeV oxygen ions. The branching ratios for the de-excitation of levels in the ground-state rotational bands were determined by measuring the γ -ray intensities in singles spectra observed with a Ge(Li) detector. $M1$ transition rates were obtained from the branching ratios with the assumption that the rotational-model predictions for the $E2$ transition rates are correct. For ^{159}Tb , six $M1$ transition rates are compared. In all cases the $M1$ transition rates agree with rotational-model theory within experimental error. Absolute $E2$ transition rates were also measured for some of the vibrational and intrinsic states observed.

I. INTRODUCTION

THE Bohr-Mottelson rotational model^{1,2} predicts that the relative $E2$ and $M1$ transition probabilities in a rotational band are given in terms of angular-momentum coupling coefficients. These predictions have been verified experimentally³⁻⁷ for $E2$ transitions. Measurements^{6,8} have also been made of relative $M1$ transition rates; however, the experimental accuracies were insufficient to provide a critical test of the model. Measurements by deBoer⁸ in rare-earth nuclei indicated possible deviations from the model predictions for relative $M1$ transition rates for high spin states. Again, the accuracies of these measurements were not adequate to draw a definite conclusion.

In the present experiment much higher accuracy has been obtained by the use of a high-resolution lithium-drifted germanium detector. γ -ray branching ratios were measured in six deformed nuclei, ^{153}Eu , ^{159}Tb , ^{165}Ho , ^{169}Tm , ^{175}Lu , and ^{181}Ta , from which the relative $M1$ transition rates were obtained and compared with the model. The results have been presented in part earlier.⁹ Similar measurements have been made recently by Boehm *et al.*¹⁰ and are discussed below.

In addition to the data on ground-state rotational bands, some excitation strength of vibrational and intrinsic states was also obtained.

II. THEORY

A. Energy Levels

The energies of the levels of a rotational band are given by the following expression:

$$E_I = E_0 + (\hbar^2/2\mathcal{I})[I(I+1) + a(-1)^{I+1/2}(I+\frac{1}{2})\delta_{K,1/2}] + B[I(I+1) + a(-1)^{I+1/2}(I+\frac{1}{2})\delta_{K,1/2}]^2, \quad (1)$$

where \mathcal{I} is the effective moment of inertia of the nucleus, I is the spin of the excited level, K is the projection of the odd-particle angular momentum on the nuclear symmetry axis, and a is a decoupling parameter which occurs for $K=\frac{1}{2}$. The second term in Eq. (1) takes into account higher-order effects such as rotation-vibration interactions.

B. Transition Probabilities and Magnetic Moments

The pure rotational model of Bohr and Mottelson² describes the electromagnetic properties of a rotational band in terms of a set of four parameters g_K , g_R , Q_0 , and b_0 , where g_K and g_R are gyromagnetic ratios for intrinsic and collective motion, Q_0 is the intrinsic quadrupole moment, and b_0 is an additional parameter occurring in the relation for a magnetic dipole moment or transition when $K=\frac{1}{2}$.

The reduced $M1$ transition probability from a state $I+1$ to another state I of the same rotational band is given by

$$B(M1, I+1 \rightarrow I) = \frac{3}{4\pi} \left(\frac{e\hbar}{2M_0c} \right)^2 (g_K - g_R)^2 \times \frac{K^2(I+1-K)(I+1+K)}{(I+1)(2I+3)} \times [1 + (-1)^{I-1/2} b_0 \delta_{K,1/2}]^2. \quad (2)$$

* Work supported by the U. S. Atomic Energy Commission.

† Present address: Department of Physics, Rutgers, The State University, New Brunswick, New Jersey.

‡ Visiting Staff Member from Department of Physics, University of Texas, Austin, Texas.

§ Present address: Department of Physics, Emory University, Atlanta, Georgia.

¹ A. Bohr, Kgl. Danske Videnskab. Selskab, Mat.-Fys. Medd. 26, No. 14 (1952).

² A. Bohr and B. R. Mottelson, Kgl. Danske Videnskab. Selskab, Mat.-Fys. Medd. 27, No. 16 (1953).

³ B. Elbek, K. O. Nielsen, and M. C. Olesen, Phys. Rev. 108, 406 (1957).

⁴ M. C. Olesen and B. Elbek, Nucl. Phys. 15, 134 (1960).

⁵ J. deBoer, G. Goldring, and H. Winkler, Phys. Rev. 134, B1032 (1964).

⁶ E. M. Bernstein and R. Graetzer, Phys. Rev. 119, 1321 (1960).

⁷ A. C. Li and A. Schwartzchild, Phys. Rev. 129, 2664 (1963).

⁸ J. deBoer, California Institute of Technology Report No. CALT-63-16, 1964 (unpublished); J. deBoer and G. D. Symons, in *Proceedings of the International Congress of Nuclear Physics, Paris, 1963*, edited by P. Guenberger (National Center of Scientific Research, Paris, 1964), p. 541.

⁹ G. G. Seaman, E. M. Bernstein, and J. M. Palms, in *Proceed-*

ings of the International Conference on Nuclear Physics, Gallinburg, 1966 (to be published).

¹⁰ F. Boehm, G. Goldring, G. B. Hagemann, G. D. Symons, and A. Tvetar, Phys. Letters 22, 627 (1966).

The value of $B(M1, I+2 \rightarrow I+1)$ can be calculated from the experimental γ -ray branching ratio λ (cascade to crossover), and the ratio of $E2$ transition probabilities given in terms of transition energies and the reduced electric quadrupole transition probabilities $B(E2)$ using the following relation:

$$B(M1, I+2 \rightarrow I+1) = 6.97 \times 10^{-7} \frac{(\Delta E_2)^5}{(\Delta E_1)^3} B(E2, I+2 \rightarrow I) \times \left[\lambda - \left(\frac{\Delta E_1}{\Delta E_2} \right)^5 \frac{B(E2, I+2 \rightarrow I+1)}{B(E2, I+2 \rightarrow I)} \right]. \quad (3)$$

ΔE_1 and ΔE_2 are the energies of the $I+2 \rightarrow I$ and $I+2 \rightarrow I+1$ transitions in keV.

In the analysis of the data of the present experiment, the assumption was made that the relative $B(E2)$ values between rotational states are given correctly by the model. The $B(E2)$ values are related by

$$B(E2, I_i \rightarrow I_f) = \frac{5}{16\pi} e^2 Q_0^2 \langle I_i 2K0 | I_f 2I_f K \rangle^2. \quad (4)$$

The values of Q_0 used in this analysis were obtained from measurements of the excitation of the first excited state by Oleson and Elbek⁴ for ¹⁵³Eu, ¹⁵⁹Tb, ¹⁶⁵Ho, and ¹⁶⁹Tm, by Elbek *et al.*¹¹ for ¹⁷⁵Lu, and by Bernstein and Graetzer⁶ for ¹⁸¹Ta.

An additional $M1$ transition probability can be obtained for the decay of the first excited state when a value of δ^2 , the $E2/M1$ ratio, is known. The relation is as follows:

$$B(M1, I+1 \rightarrow I) = 6.97 \times 10^{-7} \frac{(\Delta E)^2}{\delta^2} B(E2, I+1 \rightarrow I). \quad (5)$$

III. EXPERIMENTAL PROCEDURE

A. Data Acquisition

Levels in the ground-state rotational bands studied were populated by multiple Coulomb excitation with oxygen ions, and the de-excitation γ rays were observed with a Ge(Li) detector. A 50-MeV oxygen beam produced by the Los Alamos Scientific Laboratory FN Tandem Van de Graaff was used to bombard thick, metallic targets of the nuclei studied. The target chamber and detector have been described previously.¹² All γ -ray measurements were made at 55° to the beam direction to minimize angular-distribution effects.

Thick targets of ¹⁵⁹Tb, ¹⁶⁵Ho, ¹⁶⁹Tm, and ¹⁷⁵Lu were made by evaporating a layer of material 30 to 100-mg/cm² thick onto 12.6-mg/cm² tantalum foil. This

was more than adequate to stop the beam in the target material. The ¹⁵³Eu target was produced by reducing the separated isotope in the oxide form with lanthanum in a vacuum at about 600°C and simultaneously evaporating it onto an aluminum foil. The targets were stored in a vacuum to reduce oxide formation and were cleaned mechanically prior to use.

The γ -ray detector was lithium-drifted germanium with a resolution of 3–4 keV in the region of interest and a sensitive volume of about 5 cm³. The fabrication of this detector has been reported elsewhere.¹³ The preamplifier and amplifier were of a type designed at Lawrence Radiation Laboratory. The first stage of the preamplifier was a field-effect transistor placed near the detector in the vacuum and cooled to liquid-nitrogen temperature.

The γ -ray pulses were digitized in a 2048-channel Victoreen analog-to-digital converter with a channel resolution of about 0.5-keV per channel and stored in the memory of an SDS-930 computer. The stability of the system was better than 0.05% over a typical data collecting time of 6 h, so no gain stabilization was employed. Absorbers of 0.79 mm of tin and 1.02 mm of copper were used to reduce the low-energy γ -ray counting rates. For measurements of the more intense low-energy transition intensities shorter runs were made with the tin and copper absorbers removed and with a channel resolution of about 0.25-keV per channel.

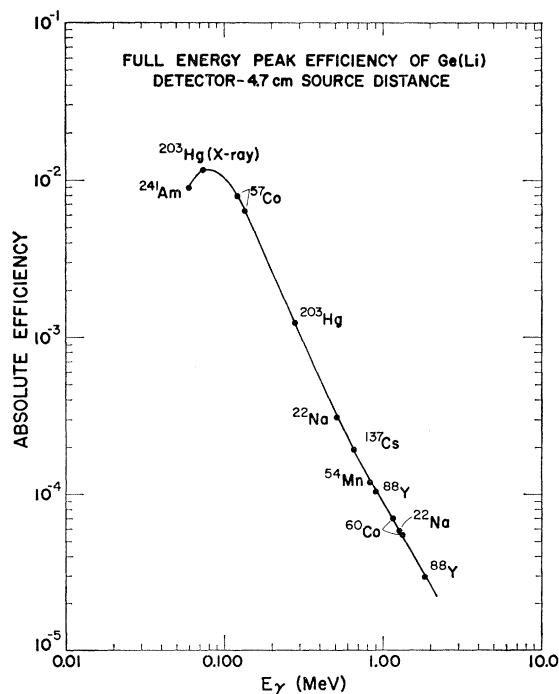


FIG. 1. Absolute full-energy peak γ -ray efficiency for the Ge(Li) detector at 4.7 cm.

¹¹ B. Elbek, M. C. Olesen, and O. Skilbreid, Nucl. Phys. 10, 294 (1959).

¹² J. M. Palms, E. M. Bernstein, and G. G. Seaman, Phys. Rev. 151, 1004 (1966).

¹³ J. M. Palms and A. H. Greenwood, Rev. Sci. Instr. 36, 1209 (1965).

Data reduction consisted of correcting γ counts in the spectra for absorption and detector efficiency. The spectra were analyzed with a computer program which made least-squares fits to the data with skewed Gaussian peaks and linear or exponential backgrounds. γ -ray absorption in the tin and copper absorbers, the target chamber, and the target was calculated from cross sections given by Wapstra.¹⁴ A check of the calculations was made in each case with a measurement of the absorption of 59.6-keV γ rays from a ²⁴¹Am source. The absolute detector efficiency (Fig. 1) at the 4.7-cm distance from target to detector face used in all measurements was made with a set of sources (²⁴¹Am, ⁵⁷Co, ²⁰³Hg, ¹⁹⁸Au, ²²Na, ¹³⁷Cs, ⁵⁴Mn, ⁶⁰Co, and ⁸⁸Y) from the International Atomic Energy Agency calibrated to $\pm 2\%$ or better. γ -ray energy calibrations were made with these same sources.

B. Calculation of Excitation Probabilities

In order to calculate excitation probabilities for some of the direct excitations, the number of incident ions was obtained by counting the elastically scattered ions in an annular ring detector while simultaneously measuring the direct γ -ray spectrum. The ratio of the number of ions to the intensity of a strong γ -ray peak was used to normalize spectra taken for long counting times with no counting of ions. The ring detector was placed at back angles with an average angle of 172° . Since the scattered-particle spectrum from a thick target extends from a maximum value down to zero energy, all particles above a certain discriminator level were counted. This discriminator level also served to determine a minimum energy in the thick target integration of the Rutherford cross section.

Yield calculations were made by integrating the cross sections from incident energy down to an energy where additions to the yield were considerably less than 1%. The expression for first-order excitation¹⁵ is (for the total cross section)

$$Y/B(E2) = (\text{No. ions}) \frac{N_{Av}}{A_2} C_{E2} \times \int_{E_{\min}}^{E_0} \frac{(E - \Delta E') f_{E2}(\xi) dE}{dE/d(\rho x)}, \quad (6)$$

where N_{Av} is Avogadro's number,

$$C_{E2} = \frac{4.79 A_1}{Z_2^2 (1 + A_1/A_2)^2}, \quad (7)$$

$$\xi = \frac{Z_1 Z_2 A_1^{1/2} \Delta E'}{12.65 (E - \frac{1}{2} \Delta E')^{3/2}}, \quad (8)$$

and f_{E2} is tabulated in Ref. 15. Subscripts 1 and 2 denote projectile and target, respectively, and energies E , ΔE (excitation energy), and $\Delta E' = (1 + A_1/A_2)\Delta E$ are in MeV.

The $dE/d(\rho x)$ values for oxygen ions were based on the data of Booth and Grant.¹⁶ Their measurements extend from 2 to only 24 MeV, but the reciprocal of $dE/d(\rho x)$ is very nearly linear with energy from 12 to 24 MeV and can therefore be extrapolated to higher energies. The semiempirical relationships of Hubbard¹⁷ and Northcliffe¹⁸ show that this linear extrapolation is valid to 80 MeV. The expression used for the targets here is a linear interpolation between measurements in Ag and Au:

$$\frac{1}{dE/d(\rho x)} = \frac{Z-47}{32} (0.109 - 0.0005E) + (0.222 + 0.004E) \frac{\text{mg/cm}^2}{\text{MeV}}, \quad (9)$$

where Z is the atomic number of the target nucleus, and E is the oxygen ion energy in MeV.

C. Discussion of Errors

Errors in the γ -ray intensities are due largely to background subtraction uncertainties. The relative efficiency errors are $\pm 4\%$ above 100 keV and somewhat higher below that where the efficiency curve (Fig. 1) turns over. Errors in the γ -ray energies are estimated as ± 0.3 keV up to 511 keV and ± 0.5 keV above that. For very weak γ rays the errors are estimated as ± 1 keV, which is indicated by omission of a decimal point in the quoted energy.

The effect of γ -ray angular distributions on the data is expected to be small because the counter was placed at an angle of 55° to the beam direction where the second-order Legendre polynomial P_2 in the usual expression¹⁵

$$W(\theta_\gamma) = 1 + a_2 A_2 P_2(\cos\theta_\gamma) + a_4 A_4 P_4(\cos\theta_\gamma) \quad (10)$$

is zero. Further, the coefficients A_2 and A_4 decrease with increasing spin, and thus only transitions between the first few states in the nuclei with low ground-state spins might have appreciable anisotropies. In this experiment anisotropies would be expected to be largest in ¹⁶⁹Tm and ¹⁵⁹Tb, with ground-state spins of $\frac{1}{2}$ and $\frac{3}{2}$, respectively. Measurements were made of the angular distribution of γ rays from the decay of the $\frac{7}{2}$ 137.5-keV level in ¹⁵⁹Tb and no large anisotropies were observed. Therefore all angular-correlation effects have been neglected.

¹⁴ A. H. Wapstra, G. J. Nijgh, and R. von Lieshout. *Nuclear Spectroscopy Tables* (North-Holland Publishing Company, Amsterdam, 1959).

¹⁵ K. Alder, A. Bohr, T. Huus, B. Mottelson, and A. Winther, *Rev. Mod. Phys.* **28**, 432 (1956).

¹⁶ W. Booth and I. S. Grant, *Nucl. Phys.* **63**, 481 (1965).

¹⁷ E. L. Hubbard, University of California Report No. UCRL-9053, 1960 (unpublished).

¹⁸ L. C. Northcliffe, *Ann. Rev. Nucl. Sci.* **13**, Appendix B (1963).

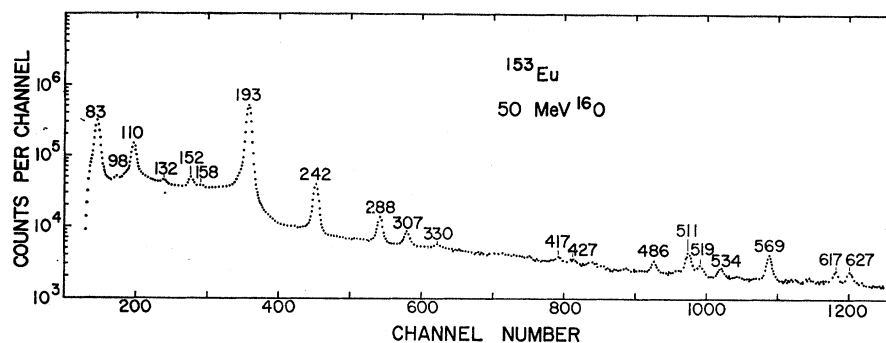


FIG. 2. Ge(Li) singles spectrum for 50-MeV oxygen ions on ^{153}Eu .

IV. DECAY SCHEMES

The ground-state rotational band transitions are easily identified because of their strong intensities and characteristic energy sequence. In the nuclei studied here all of the ground-state band transitions are less than 511 keV, and most of the vibrational and intrinsic state transitions are of higher energy. Most of the levels have been determined in earlier heavy-ion investigations^{8,19,20} and have been confirmed here. The data are presented in Figs. 2–8, and the γ -ray energies and levels are given in the decay schemes in Figs. 9–13. The level energies are also given in Table I. The parameters of Eq. (1) are given in the table, and the calculated level energies are compared with the experimental. The level assignments are usually based on two energy sums as well as qualitative intensity arguments. Energies from previous experiments are given in parentheses in Table I.

A. Europium-153

The γ -ray spectrum of ^{153}Eu is very complex, and there is very little agreement between the γ -ray spectra

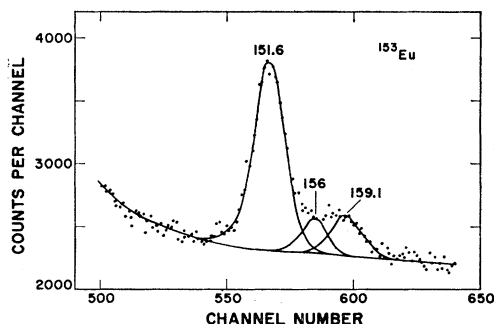


FIG. 3. Detail of ^{153}Eu singles spectrum.

observed here and those from the β decay^{20,21} of ^{153}Sm . There is a 2-keV difference in the energy of the second rotational state ($\frac{9}{2}^+$), but it appears only very weakly in β decay and is very strong here (see Fig. 2). Further, very few intrinsic states are populated by Coulomb excitation, and, conversely, very few vibrational states are populated in β decay.

The calculation of the ground-state band level energies from Eq. (1) is given in Table I, and it is seen that the higher levels are not well predicted. A similar situation exists²² in the neighboring nucleus ^{152}Sm , which also has 90 neutrons and has a highly perturbed ground-state band.

The ground-state rotational band includes transitions up to 330 keV in energy (see Fig. 2). The 98- and 152-keV γ rays are from intrinsic states, and the 307 keV is from a small impurity of ^{151}Eu in the target. The γ rays at 417, 427, and 511 keV are from oxygen reactions with target surface contaminants. These γ rays and additional ones at about 440, 695, and 709 keV are common to all targets in varying degrees.

In earlier branching-ratio data⁸ obtained with a NaI(Tl) detector, the 152- and 159-keV transitions were unresolved from the very low-intensity 156-keV de-excitation of the $(13/2)^+$ level, yielding an anomalous branching ratio. This region is shown in detail in Fig. 3. The proper choice of γ ray is made on the basis of the energy of the $(13/2)^+$ level, obtained within 0.3 keV from the more intense 287.9-keV crossover transition. The level structure is given in Fig. 9. The origin of the 159-keV γ ray is not known.

None of the strong γ rays at 486 keV and above have been observed in other work.^{20,21} Some tentative level assignments may be made on the basis of energy sums. As shown in Fig. 9, four of the γ rays sum conveniently to yield two levels at 568.9 and 617.9 and 617.5 keV. It is tempting to assign these to the same band. If one assumes that they belong to a γ -vibrational band, the $\frac{1}{2}^+$ band is ruled out by the 485.5-keV transition.

¹⁹ J. S. Greenberg, D. A. Bromley, G. G. Seaman, and E. V. Bishop, in *Proceedings of the Third Conference on Reactions Between Complex Nuclei, Asilomar, 1963*, edited by A. Ghiorso, R. M. Diamond, and H. E. Conzett (University of California Press, Berkeley, 1963), p. 295.

²⁰ *Nuclear Data Sheets*, compiled by K. Way *et al.* (Printing and Publishing Office, National Academy of Sciences—National Research Council, Washington 25, D. C.).

²¹ P. H. Blichert-Toft, E. G. Funk, and J. W. Mihelich, *Nucl. Phys.* **79**, 12 (1966).

²² G. G. Seaman, J. S. Greenberg, D. A. Bromley, and F. K. McGowan, *Phys. Rev.* **149**, 925 (1966).

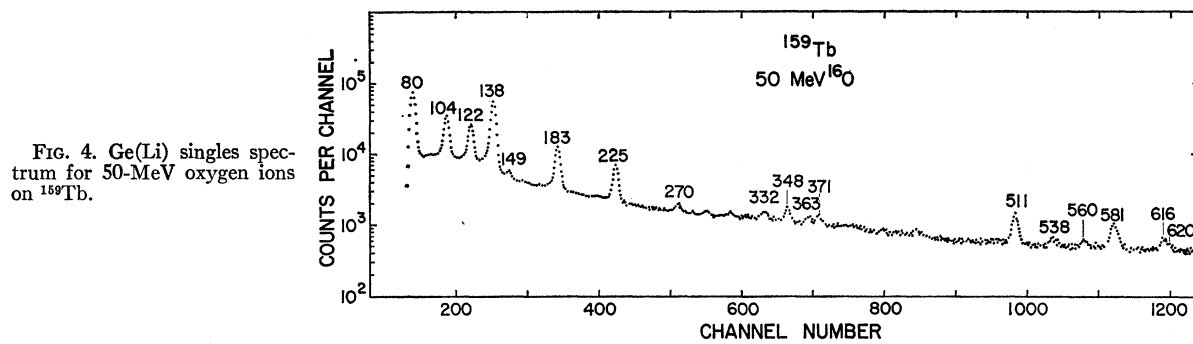


FIG. 4. Ge(Li) singles spectrum for 50-MeV oxygen ions on ¹⁵⁹Tb.

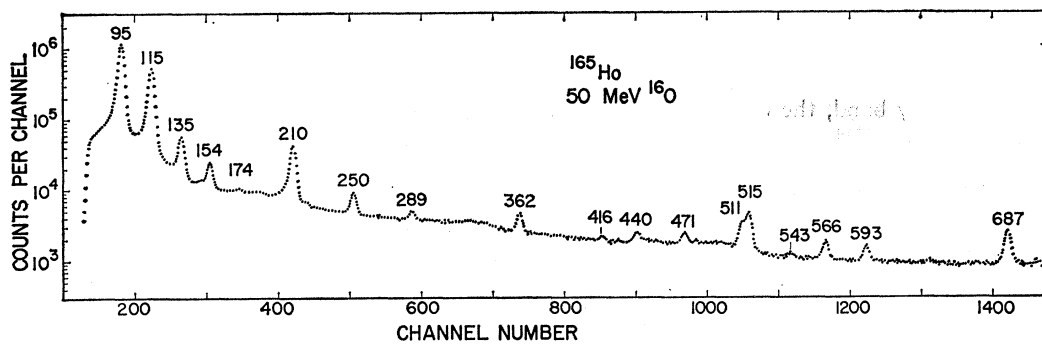


FIG. 5. Ge(Li) singles spectrum for 50-MeV oxygen ions on ¹⁶⁵Ho.

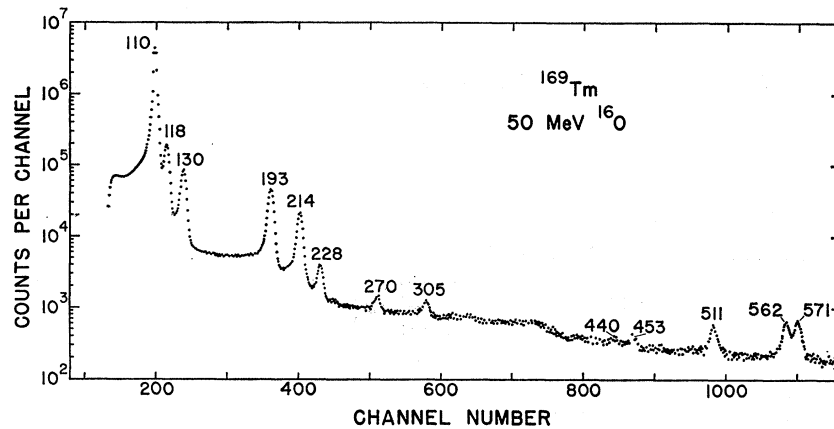


FIG. 6. Ge(Li) singles spectrum for 50-MeV oxygen ions on ¹⁶⁹Tm.

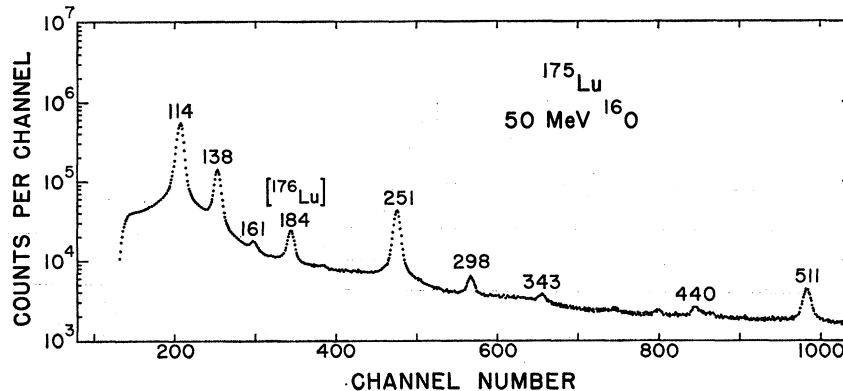


FIG. 7. Ge(Li) singles spectrum for 50-MeV oxygen ions on ¹⁷⁵Lu.

E. Lutetium-175, 176

In ^{175}Lu there appears to be no vibrational- or intrinsic-state excitation. The only complexity is from several transitions in the ground-state band of ^{176}Lu , which is 2.6% abundant in the natural lutetium target. The ^{176}Lu transitions are labeled in Fig. 7. The decay scheme is shown in Fig. 13.

F. Tantalum-181

The tantalum spectrum (Fig. 8) similarly exhibits no vibrational state excitation, but has one intrinsic state at 482 keV ($\frac{5}{2}^+$). The ground-state band transitions are intense and well separated, allowing accurate determination of the branching ratios. The decay scheme is shown in Fig. 13.

V. RESULTS AND DISCUSSION

A. Ground-State Rotational Bands

The branching ratios obtained for the ground-state rotational bands are given in Table II. The data from ^{171}Yb and ^{173}Yb in an earlier publication¹² has also been included for the sake of comparison. As mentioned above, $B(M1)$ values can be obtained for the first

excited state from values of δ^2 , and these are listed in the last column for the cases in which they are known with reasonable accuracy.

Branching ratios from other experiments are also given. The early measurements of deBoer⁸ with NaI(Tl) showed large deviations from the model, but the branching ratios are not confirmed when a higher-resolution detector is used. The measurements by Boehm *et al.*¹⁰ are in substantial agreement with those in this experiment, although their values are usually slightly larger than ours.

The values of $B(M1)$ and $|g_K - g_R|$ derived from Eq. (2) are given in Table III. The $|g_K - g_R|$ values from ^{169}Tm and ^{171}Yb are inseparable from the factor $1 - b_0$ and $1 + b_0$. Although b_0 can in principle be obtained since there is an alternation in sign for successive states, experimentally it was only possible to measure every other branching ratio. The test of the rotational model is the degree to which $|g_K - g_R|$ is constant for all states. In column 4 of the table it is seen that the values are nearly all within the experimental error compared to the average. In the last column the ratio of each value to the weighted average is given, and it is noted that the fluctuations about unity are usually within the experimental error. The agreement for ^{169}Tb ,

TABLE II. Branching ratio and δ^2 measurements.

Nuclide	Q_0 (barns)	$I_i \rightarrow I_f$	Cascade E_γ (keV)	Present exp.	deBoer ^b	λ (cascade/crossover) ^a Boehm <i>et al.</i> ^c	Others	δ^2
^{158}Eu	6.94	$7 \rightarrow 5$	83.4					0.67 (18) ^d
		$9 \rightarrow 7$	110.0	0.385(8)	0.418(15)	0.454(8)	0.352(6) ^e	
		$11/2 \rightarrow 9/2$	132.0	0.151(9)	0.42 (20)	0.141(11)		
^{159}Tb	7.41	$13/2 \rightarrow 11/2$	156.0	0.088(21)	0.93 (60)			0.015(27) ^f
		$5 \rightarrow 3$	58.0					
		$7 \rightarrow 5$	79.5	6.84 (10)	3.85 (15)	7.20 (4)	6.90 (17) ^g	
		$9 \rightarrow 7$	104.2	2.21 (10)	3.45 (20)	2.86 (9)		
		$11/2 \rightarrow 9/2$	121.5	1.49 (10)	1.85 (20)			
^{165}Ho	7.56	$13/2 \rightarrow 11/2$	148.5	0.91 (18)				
		$15/2 \rightarrow 13/2$	158.3	0.72 (28)				
		$11/2 \rightarrow 9/2$	115.1	7.30 (10)	5.55 (16)	8.93 (5)	6.74 ^h	
		$13/2 \rightarrow 11/2$	135.1	3.66 (10)	3.7 (25)	4.0 (20)	4.16 ^h	
		$15/2 \rightarrow 13/2$	154.0	2.30 (17)	2.6 (50)		2.99 ^h	
^{169}Tm	7.52	$17/2 \rightarrow 15/2$	173.4	1.4 (29)				
		$5 \rightarrow 3$	109.7	9.08 (18)		9.85 (10)		
		$7 \rightarrow 5$	193.0	1.77 (9)		2.1 (4)		
^{171}Yb	7.96	$13/2 \rightarrow 11/2$	269.5	0.785(10)				0.45 (18) ⁱ
		$3 \rightarrow 1$	67.2					
^{173}Yb	7.77	$11/2 \rightarrow 9/2$	154.8	0.433(6)		0.397(10)		
		$7 \rightarrow 5$	240.7	0.164(24)				
		$9 \rightarrow 7$	100.3	3.02 (8)		3.72 (6)	3.33 (7) ^e	
^{175}Lu	7.45	$11/2 \rightarrow 9/2$	122.2	1.43 (12)		1.56 (8)		
		$13/2 \rightarrow 11/2$	143.7	0.730(14)				
		$9 \rightarrow 7$	113.8					
^{181}Ta	6.88	$11/2 \rightarrow 9/2$	137.7	1.21 (12)	1.05 (18)	1.50 (4)	1.05 (6) ^e	0.176(22) ^d
		$13/2 \rightarrow 11/2$	160.6	0.457(14)	1.69 (60)	0.555(12)		
		$9 \rightarrow 7$	136.2					
		$11/2 \rightarrow 9/2$	165.2	1.72 (9)		1.59 (6)	1.44 (7) ^e	0.190(10) ^d
		$13/2 \rightarrow 11/2$	193.8	0.717(9)		0.621(4)		
		$15/2 \rightarrow 13/2$	221.5	0.454(12)				

^a Percent errors are given in parentheses.

^b Reference 8.

^c Reference 10.

^d Reference 6.

^e G. Goldring, H. M. Loebenstein, and R. Barloutaud, *Phys. Rev.* **127**, 2151 (1962).

^f H. Ryde, L. Persson, and K. Oelsner-Ryde, *Arkiv Fysik* **23**, 195 (1963).

^g M. Martin, P. Marmaier, and J. deBoer, *Helv. Phys. Acta* **31**, 435 (1958).

^h Calculated from $B(M1)$ values of I. Berson *et al.*, *Transactions of the Sixteenth Conference on Nuclear Spectroscopy, Moscow, 1966* (unpublished).

ⁱ R. S. Dings, W. L. Talbert, Jr., and M. G. Stewart, *Nucl. Phys.* **83**, 545 (1966).

TABLE III. Values of $B(M1)$ and $|g_K - g_R|$.

Nuclide	$I_i \rightarrow I_f$	$B(M1, I_i \rightarrow I_f)^a$	$ g_K - g_R ^b$	$ g_K - g_R / g_K - g_R _{av}$
¹⁵³ Eu	$\frac{1}{2} \rightarrow \frac{3}{2}$	0.0124(18) ^c	0.197(9)	1.10
	$\frac{3}{2} \rightarrow \frac{5}{2}$	0.0136(15)	0.171(7)	0.96
	$\frac{11}{2} \rightarrow \frac{9}{2}$	0.0171(17)	0.178(9)	1.00
	$\frac{13}{2} \rightarrow \frac{11}{2}$	0.0188(22)	0.178(11)	1.00
¹⁵⁹ Tb	$\frac{5}{2} \rightarrow \frac{3}{2}$	0.292 (27)	1.43 (14)	1.07
	$\frac{7}{2} \rightarrow \frac{5}{2}$	0.359 (10)	1.37 (5)	1.02
	$\frac{9}{2} \rightarrow \frac{7}{2}$	0.325 (10)	1.23 (5)	0.92
	$\frac{11}{2} \rightarrow \frac{9}{2}$	0.454 (10)	1.41 (5)	1.05
	$\frac{13}{2} \rightarrow \frac{11}{2}$	0.417 (18)	1.33 (9)	0.99
	$\frac{15}{2} \rightarrow \frac{13}{2}$	0.550 (28)	1.51 (14)	1.12
¹⁶⁵ Ho	$\frac{11}{2} \rightarrow \frac{9}{2}$	0.542 (10)	0.825(5)	0.96
	$\frac{13}{2} \rightarrow \frac{11}{2}$	0.755 (10)	0.885(5)	1.03
	$\frac{15}{2} \rightarrow \frac{13}{2}$	0.894 (17)	0.912(8)	1.06
	$\frac{17}{2} \rightarrow \frac{15}{2}$	0.846 (29)	0.859(15)	1.00
			0.862(3) ^d	
¹⁶⁹ Tm	$\frac{7}{2} \rightarrow \frac{5}{2}$	0.121 (18)	2.25/(1 - b_0) (9)	1.08
	$\frac{9}{2} \rightarrow \frac{7}{2}$	0.120 (9)	2.13/(1 - b_0) (5)	1.02
	$\frac{13}{2} \rightarrow \frac{11}{2}$	0.106 (13)	1.96/(1 - b_0) (7)	0.94
			2.09/(1 - b_0) (4) ^d	
¹⁷¹ Yb	$\frac{5}{2} \rightarrow \frac{3}{2}$	0.0087(18)	0.661/(1 + b_0) (9)	0.96
	$\frac{7}{2} \rightarrow \frac{5}{2}$	0.0127(7)	0.694/(1 + b_0) (4)	1.00
	$\frac{11}{2} \rightarrow \frac{9}{2}$	0.0143(28)	0.726/(1 + b_0) (14)	1.05
¹⁷³ Yb	$\frac{7}{2} \rightarrow \frac{5}{2}$	0.217 (8)	0.683(4)	0.99
	$\frac{11}{2} \rightarrow \frac{9}{2}$	0.291 (12)	0.723(6)	1.04
	$\frac{13}{2} \rightarrow \frac{11}{2}$	0.278 (14)	0.685(7)	0.99
			0.692(3) ^d	
¹⁷⁵ Lu	$\frac{7}{2} \rightarrow \frac{5}{2}$	0.096 (22)	0.430(11)	1.19
	$\frac{11}{2} \rightarrow \frac{9}{2}$	0.109 (15)	0.370(7)	1.02
	$\frac{13}{2} \rightarrow \frac{11}{2}$	0.106 (17)	0.332(8)	0.92
¹⁸¹ Ta	$\frac{5}{2} \rightarrow \frac{3}{2}$	0.109 (10)	0.363(5) ^d	
	$\frac{11}{2} \rightarrow \frac{9}{2}$	0.199 (10)	0.458(5)	0.95
	$\frac{13}{2} \rightarrow \frac{11}{2}$	0.224 (10)	0.500(5)	1.04
	$\frac{15}{2} \rightarrow \frac{13}{2}$	0.264 (15)	0.482(5)	1.00
			0.496(8)	1.03
		0.482(3) ^d		

^a In units of $(e\hbar/2M_p c)^2$. ^b In units of $e\hbar/2M_p c$. ^c Percent errors are given in parentheses. ^d Weighted average.

in which there are values for six successive states, indicate no evidence for deviations from the rotational-model predictions.

The Coriolis coupling discussed in Sec. IV might be expected to produce spin-dependent effects on the $M1$ transition ratio. However, Kerman²⁴ has shown that the effect of Coriolis coupling is to add a constant to $|g_K - g_R|$, thus preserving the spin dependence given in Eq. (2).

B. Excitation of Vibrational and Intrinsic States

The excitation of vibrational and intrinsic states has been expressed in terms of $B(E2)$ values calculated from first-order perturbation theory. This is not strictly correct, since higher-order excitation mechanisms, such as transitions within either the ground state or the vibrational band coupled with the interband transition, can contribute to the yield. Lütken and Winther²⁵ have considered such processes and have found that

TABLE IV. Excitation of vibrational and intrinsic states.

Nuclide	Parent level E (keV)	Transition $I\pi$	E_γ (keV)	$\epsilon B(E2)$ [$e^2 \times 10^{-48} \text{ cm}^4$] ^a
¹⁵³ Eu	568.9		485.5	0.0097 (13)
			568.9	0.34 (12)
	617.5		534.1	0.0099 (14)
			617.5	0.0143 (14)
¹⁵⁹ Tb	347.9	$\frac{5}{2}^+$	347.9	0.00375 (13)
	363.0	$\frac{7}{2}^-$	363.0	0.00304 (17)
	429.0	$\frac{3}{2}^+$	371.0	0.00400 (17)
	580.5	$\frac{1}{2}^+$	580.5	0.0227 (13)
	617.0	$\frac{3}{2}^+$	560.0	0.00525 (26)
			617.0	0.00705 ^b (21)
¹⁶⁵ Ho	675.0	$\frac{5}{2}^+$	617.0	0.00823 ^c (21)
	515.0	$\frac{3}{2}^-$	515.0	0.0363 (12)
	566.6	$\frac{7}{2}^-$	471.9	0.00768 (10)
			566.5	0.0126 (9)
	637.0	$\frac{7}{2}^-$	543.0	0.00248 (22)
	688.6	$(11/2)^-$	478.8	0.00215 (18)
			593.8	0.138 (9)
¹⁶⁹ Tm	571.0	$\frac{3}{2}^+$	688.6	0.0560 (9)
			452.8	0.00245 (10)
			562.7	0.0132 (10)
¹⁸¹ Ta	482.0	$\frac{5}{2}^+$	571.0	0.0167 (13)
			482.0	0.00148 (15)
			482.0	0.00148 (15)

²⁴ A. K. Kerman, Kgl. Danske Videnskab. Selskab, Mat.-Fys. Medd. **30**, No. 15 (1955).

²⁵ H. Lütken and A. Winther, Kgl. Danske Videnskab. Selskab, Mat.-Fys. Skrifter **2**, No. 6 (1964).

^a Percentage errors are given in parentheses.
^b Calculated with full intensity of 617-keV γ rays assigned to 617-keV level.
^c Calculated with full intensity of 617-keV γ rays assigned to 675-keV level.

the excitation of the band head alone by a first-order process is the same as the sum of the excitation to all levels in the band. Thus, the sum of the partial $B(E2)$ values, $\epsilon B(E2)$, gives a measure of the strength of the vibrational excitation.

In Table IV the $\epsilon B(E2)$ values are given for the γ -ray transitions whose intensities could be measured with reasonable accuracy and whose assignment was reasonably certain. Both the γ -ray energy and the parent level are listed in the table.

There are some discrepancies between the results obtained here and those obtained by Diamond *et al.*²³ This may be due in part to their use of higher-beam energies which may be close enough to the Coulomb

barrier so that the Coulomb excitation theory is not correct. Some of the discrepancies might also be due to uncertainties in the $E2$ to $M1$ mixing ratios assumed by Diamond *et al.*²³ It is necessary for these authors to know the mixing ratios in order to calculate γ -ray yields from their conversion-electron data.

ACKNOWLEDGMENTS

The authors wish to thank Dr. H. T. Motz for helpful discussions, Dr. R. L. Henkel and Dr. R. H. Woods of the Los Alamos tandem Van de Graaff for providing the oxygen beams used in this experiment, and Larry Allen and Judith Gursky for fabricating the targets.

Low-Energy Spectra of Odd-Mass Tc and Ru Isotopes

A. GOSWAMI*

Department of Physics, Case Institute of Technology and Western Reserve University, Cleveland, Ohio

AND

A. I. SHERWOOD†

Centre D'Etudes Nucléaires De Saclay, Seine et Oise, France

(Received 10 April 1967)

A possible explanation is given for the "anomalous" low-lying levels of the odd-mass Tc isotopes in terms of the theory of extended quasiparticle-phonon coupling, with the prediction of low-lying high-spin levels. It is checked that the same parameters used in the Tc calculation give a reasonable fit to the low-energy spectra of Ru isotopes. In particular, these calculations account for the anomalous high density of low-lying states in the Ru isotopes.

1. INTRODUCTION

THE low-energy spectra of odd-mass Tc isotopes exhibit several interesting features. Firstly, the existence of a low-lying $\frac{7}{2}^+$ state is well known.¹ A low-lying $\frac{5}{2}^+$ level has also been seen² in Tc⁹⁹ and possibly in Tc⁹⁷. The character of these levels cannot be predominantly single quasiparticle since the $g_{7/2}$ and $d_{5/2}$ (shell model) level energies are too high (being in the next major shell) compared with the $g_{9/2}$ level which is filling up. Kisslinger³ and also Talmi⁴ have suggested that the $\frac{7}{2}^+$ levels can be attributed to a $(g_{9/2})^3_{7/2}$ three-quasiparticle configuration. It is well known, for example, that for V⁵¹, this type of configuration $[(f_{7/2})^3_{5/2}]$ is substantially lowered in energy by

the residual particle interaction. One should note, however, that the unperturbed energy for this state is at least 1.5 MeV higher than the $g_{9/2}$ quasiparticle state. It is, therefore, very doubtful that by this mechanism the low-lying $\frac{7}{2}^+$ state could predominantly be the three-quasiparticle state discussed above. Moreover, such a description would still leave the low-lying $\frac{5}{2}^+$ levels unaccounted for. However, the quasiparticle-phonon coupling (QPC) calculations of Kisslinger and Sorensen⁵ (hereafter referred to as KS) show that the phonon-type levels also appear ~ 1 MeV too high.

Secondly, the $\frac{9}{2}^+$ level is usually the ground state (except possibly for Tc¹⁰¹) and the $\frac{1}{2}^-$ level appears as a very low-lying excited state. In the KS calculation, the $\frac{9}{2}^+$ level moves very rapidly and appears much higher than the $\frac{1}{2}^-$ level in Tc⁹⁷, Tc⁹⁹, and Tc¹⁰¹. This defect of the KS calculation is in part due to the neglect of self-consistency in the choice of the single-particle energies.

Thirdly, the other low-lying negative-parity levels

* Work partially supported by the National Science Foundation.

† Supported by the Atomic Commission, France.

¹ *Nuclear Data Sheets*, compiled by K. Way *et al.* (Printing and Publishing Office, National Academy of Sciences—National Research Council, Washington 25, C. D.).

² T. Cretzu and K. Hohmuth, *Nucl. Phys.* **66**, 398 (1955).

³ L. S. Kisslinger, *Nucl. Phys.* **78**, 341 (1966).

⁴ I. Talmi, in *Lectures in Theoretical Physics, VIII*, edited by W. Brittin (University of Colorado Press, Boulder, Colorado, 1965).

⁵ L. Kisslinger and R. Sorensen, *Rev. Mod. Phys.* **35**, 853 (1963).